Vlasov simulations of strongly nonlinear electrostatic oscillations in a one-dimensional electron-ion plasma

Francesco Califano[1] and Maurizio Lontano[2]
[1]*Istituto Nazionale Fisica della Materia, Sezione A, Università di Pisa and Dipartimento di Astronomia, Università di Firenze, Italy*
[2]*Istituto di Fisica del Plasma ''Piero Caldirola,'' CNR, EURATOM-ENEA-CNR Association, Milan, Italy*
(Received 5 June 1998)

The problem of the microscopic plasma response to the excitation of large amplitude electrostatic perturbations in a two-component plasma is studied by means of the numerical integration of the Vlasov-Maxwell system. The decaying of an initial electron density perturbation as well as the plasma response to an externally applied oscillating electric field are considered for times much longer than the typical ion-plasma times. The interconnections between the microscopic particle dynamics and the macroscopic plasma density and temperature evolutions are investigated. [S1063-651X(98)02811-6]

PACS number(s): 52.35.Mw, 52.35.Qz, 52.35.Fp, 52.50.Gj

I. INTRODUCTION

In 1972, Zakharov [1] established the basis of the strong turbulence theory in a collisionless plasma [2] demonstrating the possibility of the Langmuir wave collapse as an efficient channel of energy dissipation into the electrons. The excitation of shorter and shorter spatial scales, accompanying the formation of density cavities where the electrostatic (ES) field becomes trapped, provided also a physical answer to the Langmuir condensate paradox [1,3]. A large number of theoretical investigations followed those results. They were initially based on a fluid description of the medium [4–6] and were extended also to the case of magnetized plasmas [7,8]. Later on, kinetic approaches were also attempted in order to describe dissipation processes arising when the typical scale lengths become comparable with the ES screening length [9], i.e., the electron Debye length $\lambda_{De}=\sqrt{T_e/4\pi n_e e^2}$. Among the most recent papers where the process of the Langmuir collapse is treated in the frame of a Vlasov kinetic theory, we wish to mention those by Wang *et al.* [10,11]. There, the one-dimensional Vlasov-Poisson system has been numerically integrated in order to describe the onset of the modulational instability and its evolution towards the formation of density holes where the ES energy gets trapped. The kinetic results have then been compared with those of the fluid theory used in the original paper by Zahkarov [1] and good agreement has been found up to the occurrence of the first collapse. Generally speaking, most of the investigations on this subject have been carried out for small amplitude external pump field E_0. For example, in Ref. [11] the ratio $\tilde{v}^2/v_{Te}^2 \approx 10^{-3}$, between the electron quiver velocity, $\tilde{v}=eE_0/m_e\omega_0$, and the electron thermal speed, $v_{Te}=\sqrt{2T_e/m_e}$, has been assumed. Moreover, an external pump electric field oscillating at the electron plasma frequency, i.e., $\omega_0=\omega_{pe}=\sqrt{4\pi n_e e^2/m_e}$, both for an initially isothermal case, i.e., with $T_e=T_i$, and for a nonequilibrium situation, with $T_e/T_i=10$, has been considered.

The scope of our investigation is to go beyond the regimes studied in Refs. [10] and [11], by considering very large perturbations to the system. We have numerically integrated the full Vlasov-Maxwell system for the case of a free decaying initial electron density perturbation, and for the case of an externally applied electric field. The intensity of the perturbations has been characterized by $\tilde{v}^2/v_{Te}^2$ definitely larger than unity, still remaining in a nonrelativistic regime of interaction [12]. In order to work with limited integration times, a fictitious proton to electron mass ratio of 100, instead of the actual value, has been considered. This shortens the characteristic times of the ion response, with respect to the electron evolution, by a factor 4 to 5, while maintaining two well separated time scales for the two components.

In recent years new interest in such regimes of strong wave-plasma interaction has been manifested due to the experimental observations carried out in magnetic fusion devices as well as in ionospheric plasmas. In the first case, during radiofrequency plasma heating in tokamak plasmas, a reduced accessibility of the wave energy to the central plasma has been observed together with the pump wave frequency broadening, parallel wave-vector spectral modifications, and an enhancement of the density fluctuation level at the edge [13]. On the other side, in ionospheric plasmas ES wave packets with frequency of the order of the lower hybrid frequency, accompanied by localized density depletions, have been detected by the instruments of the FREJA satellite [14]. Such observations can be qualitatively described in the framework of a fluid theory of the strong wave-plasma interaction [15].

With the aim of formulating a kinetic theory of the interaction between a strong ES perturbation and a two-component plasma, we have begun a numerical investigation of the wave-plasma interaction by means of a Vlasov electromagnetic (EM) code, starting with studying the simplest case of the evolution of finite amplitude Langmuir waves in an electron-ion one-dimensional unmagnetized plasma. Notice that, due to the almost one-dimensional plasma response which characterizes the application of radiofrequency to a magnetized plasma in some specific cases [15], the simplified model adopted here can give physical hints of quite general character, as well. Two cases have been considered: (a) the relaxation of an initially given perturbation in the form of an unbalanced electron density spatial distribution, and (b) the plasma response to an externally applied oscillat-

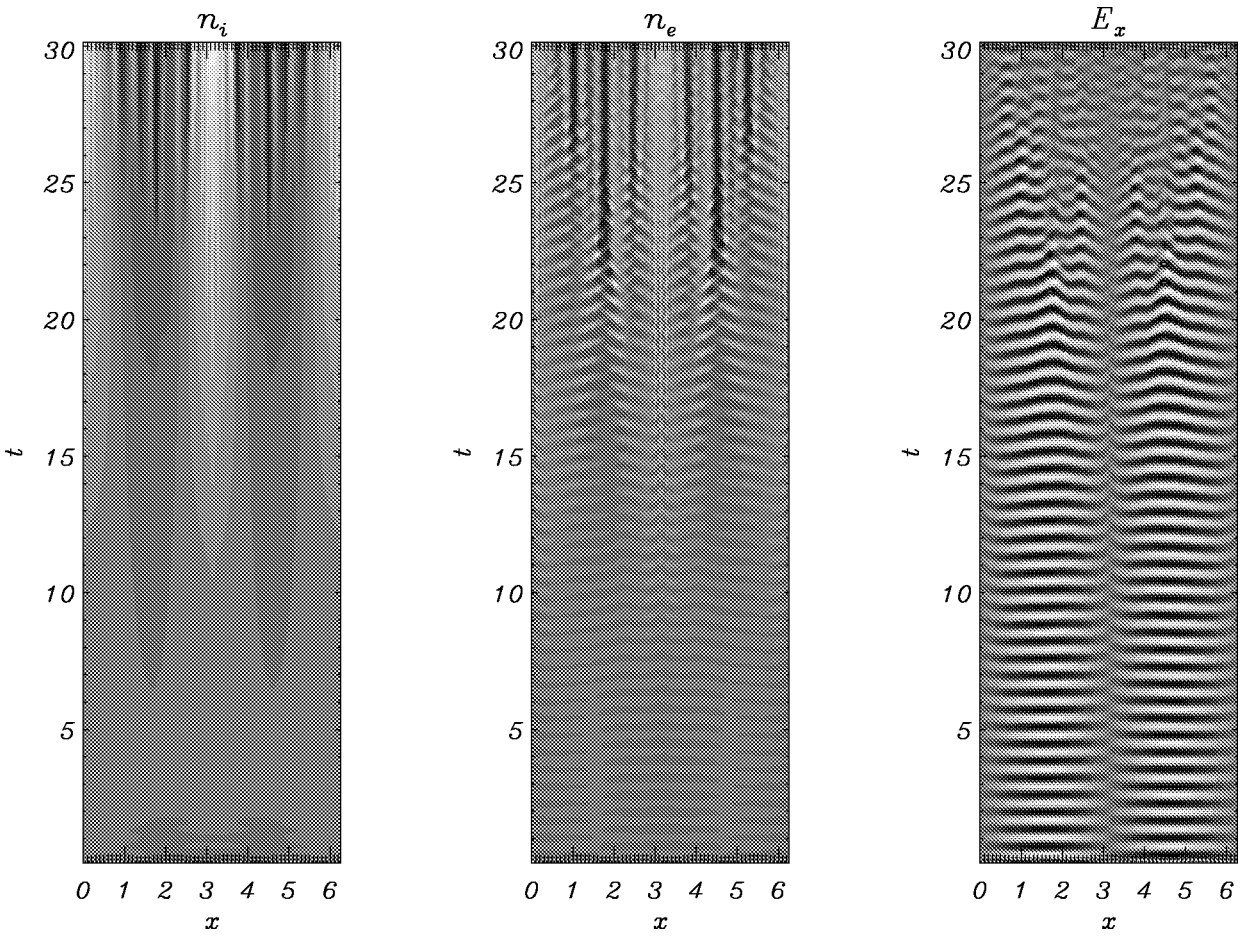

FIG. 1. The shaded contours of the spatial distributions of the ion density, of the electron density, and of the electric field are shown as functions of x and t, for the decaying plasma.

ing electric field for different values of the pump frequency ω_0.

The paper is organized as follows. In Sec. II the Vlasov-Maxwell equations relevant to our problem are written in dimensionless form. In Sec. III the relaxation of an initial electron density perturbation is studied, while Sec. IV is devoted to the plasma response to an externally applied electric field perturbation. Section V contains some concluding remarks.

II. THE MODEL

The numerical code [16] (see also [17]) solves the two Vlasov equations for two plasma species, electrons and ions, coupled with the Maxwell equations for the self-consistent fields **E** and **B**:

$$\frac{\partial f_i}{\partial t}+\mathbf{v}\cdot\frac{\partial f_i}{\partial \mathbf{r}}+(\mathbf{E}+\mathbf{v}\times\mathbf{B})\cdot\frac{\partial f_i}{\partial \mathbf{v}}=0, \tag{1}$$

$$\frac{\partial f_e}{\partial t}+\mathbf{v}\cdot\frac{\partial f_e}{\partial \mathbf{r}}-\Lambda(\mathbf{E}+\mathbf{E}_{\text{ext}}+\mathbf{v}\times\mathbf{B})\cdot\frac{\partial f_e}{\partial \mathbf{v}}=0, \tag{2}$$

$$\frac{\partial \mathbf{E}}{\partial t}=\boldsymbol{\nabla}\times\mathbf{B}-\sum_{a=e,i}\mathbf{j}_a, \tag{3}$$

$$\frac{\partial \mathbf{B}}{\partial t}=-\boldsymbol{\nabla}\times\mathbf{E}, \tag{4}$$

$$\boldsymbol{\nabla}\cdot\mathbf{B}=0, \quad \boldsymbol{\nabla}\cdot\mathbf{E}=\sum_{a=e,i}\rho_a, \tag{5}$$

where $\rho_a=q_a\int d^3v f_a(\mathbf{r},\mathbf{v},t)$ and $\mathbf{j}_a=q_a\int d^3v\,\mathbf{v} f_a(\mathbf{r},\mathbf{v},t)$ are the charge density and the current density relevant to the a species, respectively.

Equations (1)–(5) are integrated with periodic boundary conditions in $x\in[0,2\pi]$ and have been normalized according to the following rules:

$$\omega_{pi}t\to t, \quad \frac{v}{c}\to v, \quad \frac{\omega_{pi}\mathbf{r}}{c}\to\mathbf{r}, \quad \frac{m_a}{m_i}\to m_a,$$
$$\frac{f_a}{n_{0a}}\to f_a, \quad \frac{e\mathbf{E}}{m_i c\omega_{pi}}\to\mathbf{E}, \quad \frac{e\mathbf{B}}{m_i c\omega_{pi}}\to\mathbf{B}. \tag{6}$$

Here, q_a and m_a are the electric charge and the mass of the a species, c is the speed of light, e is the modulus of the electron charge, $\Lambda=m_i/m_e=100$, $\beta_a=v_{Ta}^2/c^2$, and $v_{Ta}=\sqrt{2T_a/m_a}$. T_a is the temperature of the a population. Finally, the plasma frequencies are evaluated with the unperturbed densities n_{0a} of each species. In Eq. (2), $\mathbf{E}_{\text{ext}}$ repre-

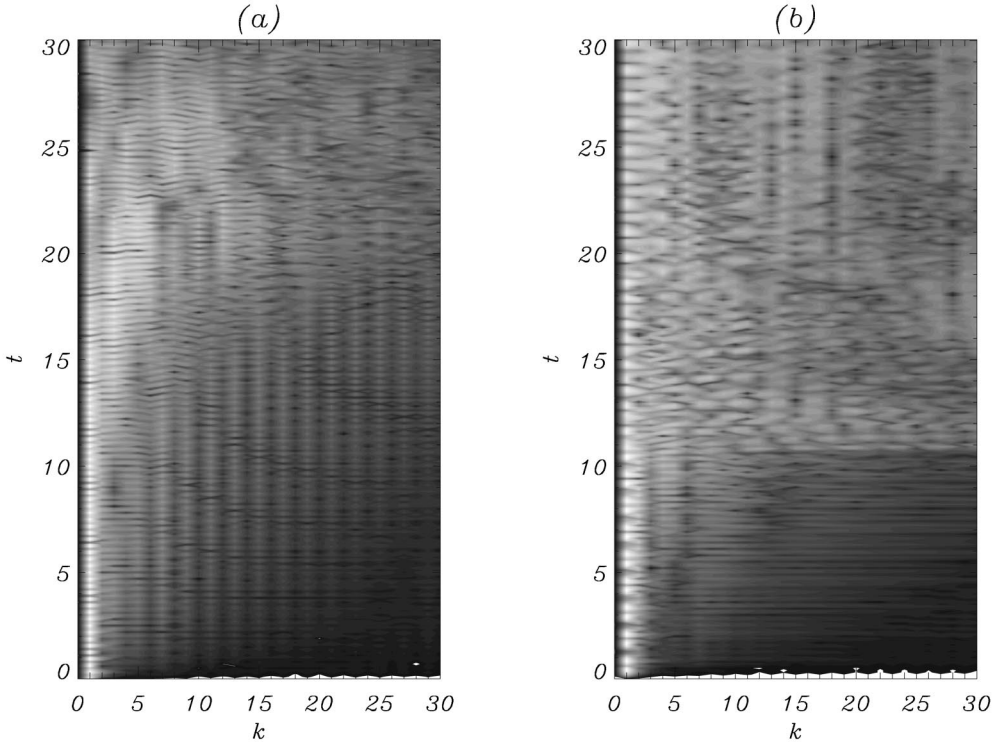

FIG. 2. The shaded contours of the k spectra of the electric field, $|E_k|^2$, as a function of k and t, for the decaying plasma (a) and for the forced case with $\omega_0=5$ (b).

sents an externally applied high-frequency electric field (if any) acting on the electron population.

The system of Eqs. (1)–(5) has been reduced to the one-dimensional case, x and $v_x(\equiv v)$ being the relevant space coordinate and velocity, respectively; furthermore, in all runs we have taken $N_x=256$, $Nv_e=500$, and $Nv_i=200$. We have limited our analysis to an initially isothermal plasma, with Maxwellian unperturbed distribution functions

$$f_i(x,v,t=0)=\frac{1}{\sqrt{\pi\beta_i}}e^{-v^2/\beta_i},$$

$$f_e(x,v,t=0)=\frac{1}{\sqrt{\pi\beta_e}}e^{-v^2/\beta_e}(1+a\ \cos x), \qquad (7)$$

$$E_x(x,t=0)=a\ \sin x,$$

where $a\geqslant 0$ is the amplitude of an initial electron density perturbation (if any) and $T_e=T_i=T$. In this paper, $\beta_e=10^{-3}$ and $\beta_i=10^{-5}$, corresponding to $T=250$ eV, have been considered. Notice that, in dimensionless quantities, $\lambda_{De}=(\beta_i T_e/T_i)^{1/2}\ll 1$.

III. THE DECAYING PLASMA

The free evolution of the physical system initially described by Eqs. (7) starting from an electric charge unbalance has been first investigated. The value $a=0.05$ used for the analysis corresponds to a ratio $\tilde{v}/v_{Te}\approx 16$ and to $\tilde{v}^2/c^2\approx 0.25$. The nonrelativistic description is then acceptable.

The initial electron density and electrostatic perturbations relax, inducing electron plasma oscillations which in the course of time create (from $t\approx 5$ to $t\approx 20$) two shallow ion density holes around the initial maxima of the electric field distribution, and then ($t>25$) develops into smaller scale microcavities, which trap ''hot spots'' of ES energy. In Fig. 1, the shaded contours of the spatial distributions of the ion density, n_i, of the electron density, n_e, and of the electric field, E_x, are shown as functions of x and t. Two different regimes of interaction can be identified. For $t<20$, the appearance of two density cavities around $x=\pi/2$ and $3\pi/2$ is observed. The formation of these broad holes follows qualitatively the law of the cavitation at small perturbation ampli-

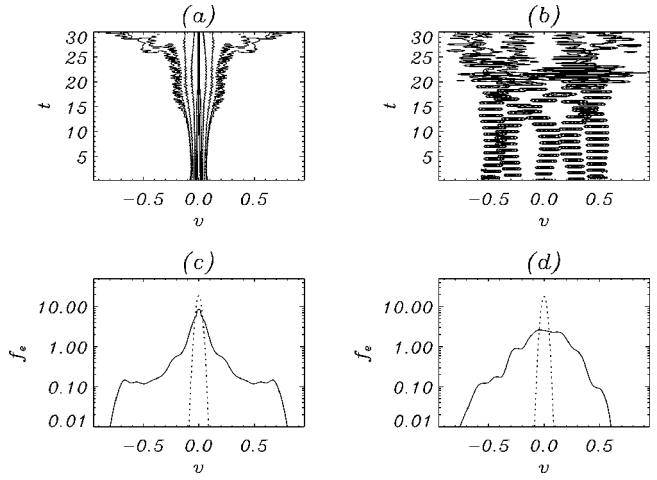

FIG. 3. The electron distribution function $f_e(x,v,t)$ for the decaying plasma. (a) and (b) show the contour lines of $f_e(x=0,v,t)$ and $f_e(x=\pi/2,v,t)$, respectively. (c) and (d) show $f_e(x=0,v,t)$ and $f_e(x=\pi/2,v,t)$ versus v, respectively, at $t=0$ (dotted lines) and $t=30$ (solid lines).

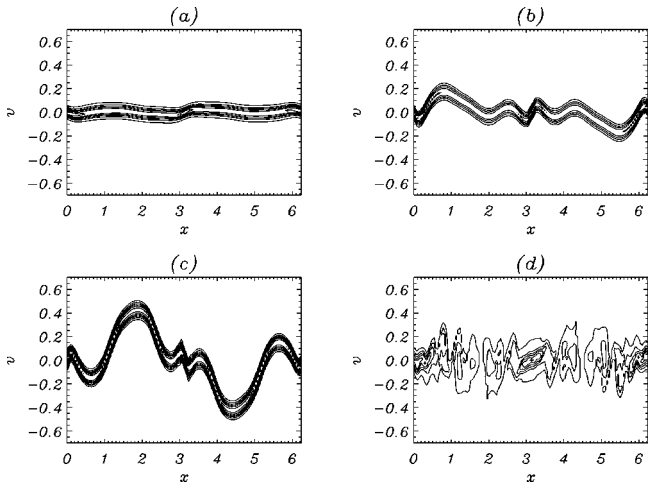

FIG. 4. The isocontours of the electron distribution function $f_e(x,v,t)$ in the phase space (x,v), for the decaying plasma. The plots refer to $t=2.7$ (a), 10.3 (b), 14.3 (c), and 30 (d).

tudes. However, at a later time, for $t>25$, a short-wavelength instability occurs, which produces a microstructure in the form of deep ion density ($|\delta n_i|/n_0 < 0.3$) troughs. The spatial scale length of this new feature remains much larger than the electron Debye length even for times much longer than those considered here. The electron density oscillates at the local electron plasma frequency around a mean value which follows the ion-density profile. The electric field oscillations are perturbed by the change of the local mean electron density and by the electrostatic energy trapped inside the density cavities. Figure 2(a) displays the k spectrum of the electric field, $|E_k|^2$, as a function of k and t, for the free decaying plasma. It is seen that the long-wavelength cavitation, occurring at $t \approx 10$, corresponds to the appearance of the lower-order odd harmonics of the initial field perturbation. Moreover, the subsequent formation of the small-scale structure in the ion-density distribution is accompanied by a strong broadening of the spectrum over a wide k interval and also by the occurrence of an appreciable harmonic overlapping.

In Fig. 3, the electron distribution function (EDF) $f_e(x,v,t)$ is studied. Plots (a) and (c) are taken at $x=0$ while plots (b) and (d) refer to $x=\pi/2$. Plots (a) and (b) show the contour lines of the EDF as a function of v and t. Plots (c) and (d) display the EDF versus v at $t=0$ (dotted lines) and $t=30$ (solid lines). A clear feature of the evolution of the electron component is that its distribution function broadens, leading to an appreciable temperature increase after $t=15-20$. As for the ions a negligible heating is observed even for longer integration times, then we can conclude that, even if at $t=0$ the plasma is isothermal and the ion-acoustic oscillations cannot be excited, during the evolution of the sys-

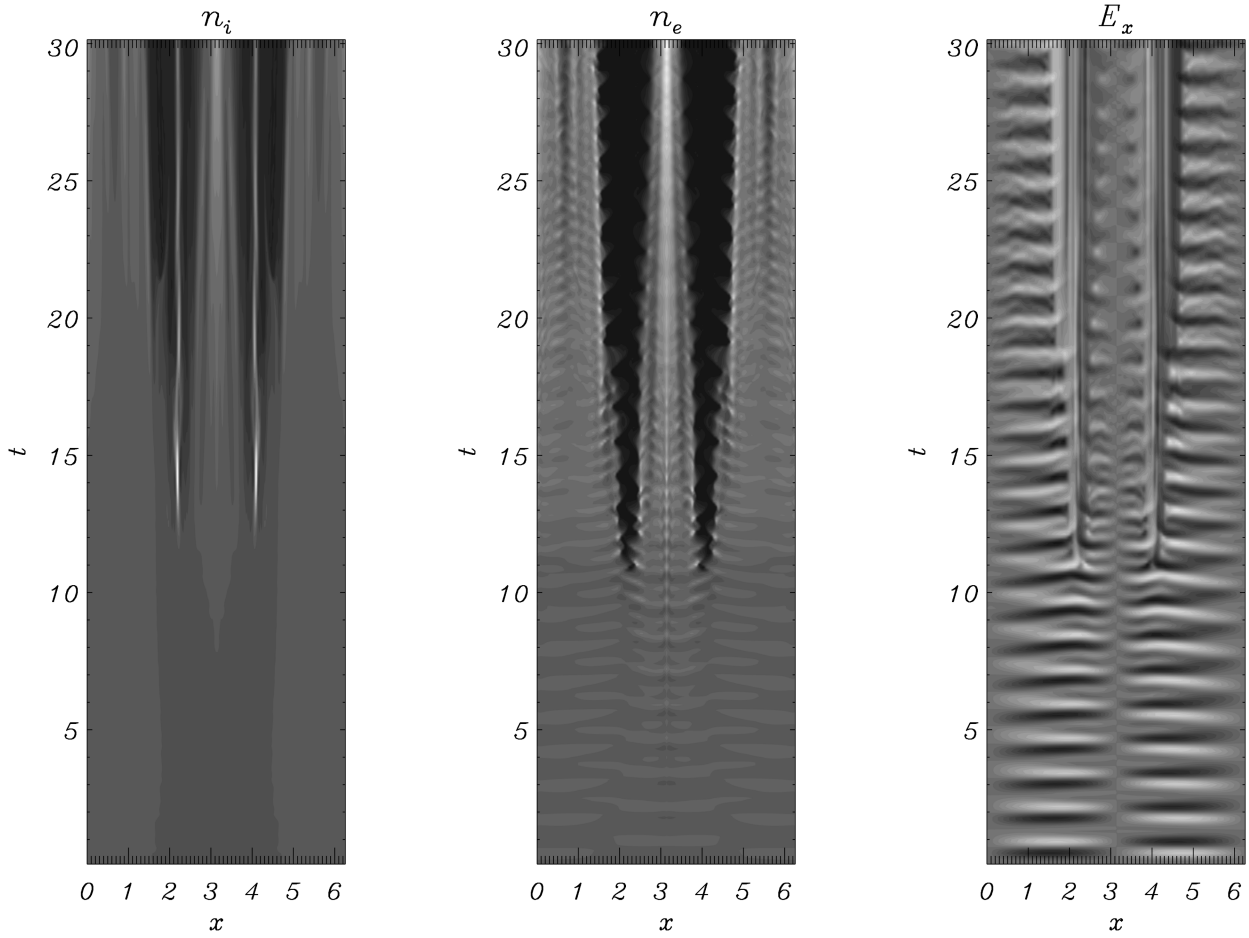

FIG. 5. The shaded contours of the spatial distributions of the ion density, of the electron density, and of the total electric field are shown as functions of x and t, for $\omega_0=5$.

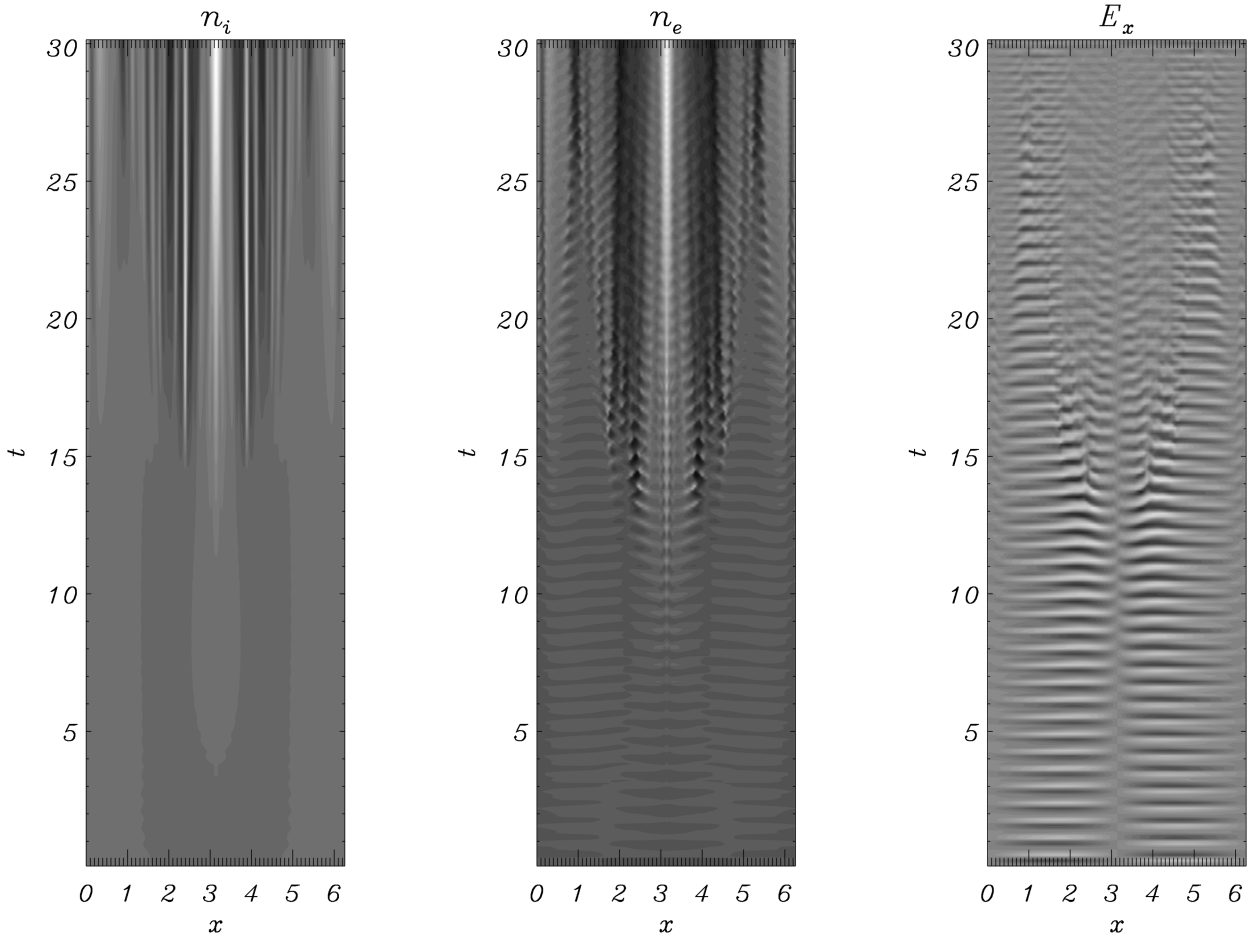

FIG. 6. The shaded contours of the spatial distributions of the ion density, of the electron density, and of the total electric field are shown as functions of x and t, for $\omega_0=20$.

tem the conditions for the existence of weakly damped ion-acoustic oscillations can be naturally realized. On the basis of a pure linear theory, we could speculate that once T_e has become appreciably larger than T_i, the plasma responds to the initial perturbation on slow time scales with the excitation of ion-acoustic oscillations. In the long-wavelength limit, i.e., for $k^2\lambda_{De}^2 \ll 1$, in dimensionless units, the time scales associated with the ion-acoustic waves are of the order of $\tau \approx 2\times 10^3$. As shown in Fig. 2(a), the range of k values excited at $t\approx 25$ extends up to $k\approx 20-30$, therefore we could expect a plasma evolution on a typical time $\tau\approx 100$. On the other side, from our numerical simulations (see Fig. 1) the time scales typical of the appearance of the microcavities in the ion density are of the order of $5-10$. This means that this phase of the evolution of the system seems to be dominated by a supersonic plasma response, which may be favored by the rapid (compared with acoustic times) formation of the ponderomotive potential.

In Fig. 4, four snapshots of the isocontours of the EDF in the phase space (x,v) are shown at $t=2.7$ (a), 10.3 (b), 14.3 (c), and 30.00 (d). It is seen that an early bunching of the EDF occurs around $x=0,\pi$, which is fed by the increase of the electric field intensity and by the lowering of the local oscillation frequency in correspondence with the density depletions. The loss of regularity of the electron oscillation in the phase space, followed by its *breaking*, leads to a kind of *electron trapping* inside the ponderomotive potential wells associated with the density structures with typical scales smaller than the wavelength of the initial perturbation. Notice that the wavebreaking of the initially nonbreaking perturbation is possible by the plasma inhomogeneity produced by the ion response [18]. In our case (that is, for $\omega\approx 10$ and $k=1$), independently of the assumed model, the resonant electron velocities do not allow an appreciable electron trapping inside the wave potential. However, we can interpret the phase structure in Fig. 4(d) as the result of a new kind of macroscopic (i.e., over several Debye lengths) electron trapping occurring when a quasistationary potential distribution is set up due to the rearrangement of the ion density under the action of the ponderomotive forces. This physical process will be discussed in more detail in the next section, where it will manifest itself more evidently.

IV. THE PLASMA RESPONSE TO AN APPLIED OSCILLATING ELECTRIC FIELD

In this section we deal with the plasma response to an externally applied oscillating electric field at the frequencies $\omega_0=5,10,20$, the value 10 corresponding to the electron plasma frequency. The relevant forcing term in Eq. (2) reads $E_{\rm ext}(x,t)=E_0\cos x\cos\omega_0 t$, where $E_0=0.05$. Due to its *resonant* character, the case with $\omega_0=10$ will be discussed separately later on. Let us first consider the two *nonresonant* cases. In Fig. 5 and in Fig. 6, the shaded contours of the ion

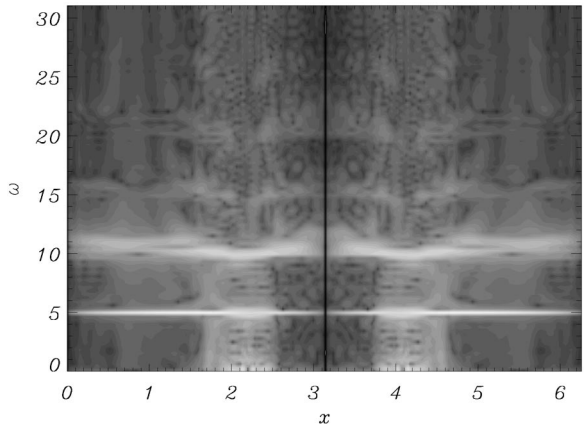

FIG. 7. The shaded contours of the frequency spectrum of the total electric field, $|E_\omega|^2$, as a function of x and ω, for $\omega_0=5$.

density, n_i, of the electron density, n_e, and of the total electric field (the pump field plus the self-consistent field), E_x, are shown as functions of x and t, for $\omega_0=5$ and 20, respectively. The continuous energy input from the external source into the electron population causes the appearance of the electron cavitation around $t\approx 13-15$, earlier than in the previous case. It is seen that, especially in the lower frequency case, the electrons are expelled quite efficiently from the regions of high field gradients. The electron plasma frequency is consequently appreciably reduced inside the cavities, while around $x=\pi$ the electrons pile up and the oscillation frequency locally increases. Figure 7 shows the shaded contours of the frequency spectrum of the electric field versus x, for $\omega_0=5$. The horizontal bright stripes at $\omega=5$ (the forcing frequency), 10 (the plasma frequency), 15, 20,... (the harmonics) are clearly visible. The horizontal structure of the plot shows that there are regions where the frequency is *upshifted* with respect to the plasma frequency, as for example for $2.6<x<3.7$, and to a less extent for $0<x<1.5$ and $4.6<x<6.3$, and regions where the frequency is *downshifted*, as for $1.5<x<2.6$ and $3.7<x<4.6$. They are the result of an average increase and lowering of the local plasma density, respectively. An interesting feature appears looking at the ion dynamics (see Figs. 5 and 6). Due to the lowering of the electron plasma frequency inside the electron cavities, the ions feel locally a quasistationary electric field, which causes them to form very sharp peaks despite the electron depletion. The possibility of creating spatial regions where the electric field is quasistationary is clearly demonstrated in the *resonant* case. In Fig. 8, the shaded contours of the ion density, electron density, and electric field are shown as functions of x and t, for $\omega_0=10$. It is seen that, whereas the electron density is almost completely expelled by the ponderomotive forces, the electric field becomes quasistationary in time. That is it oscillates over time scales which can be of the

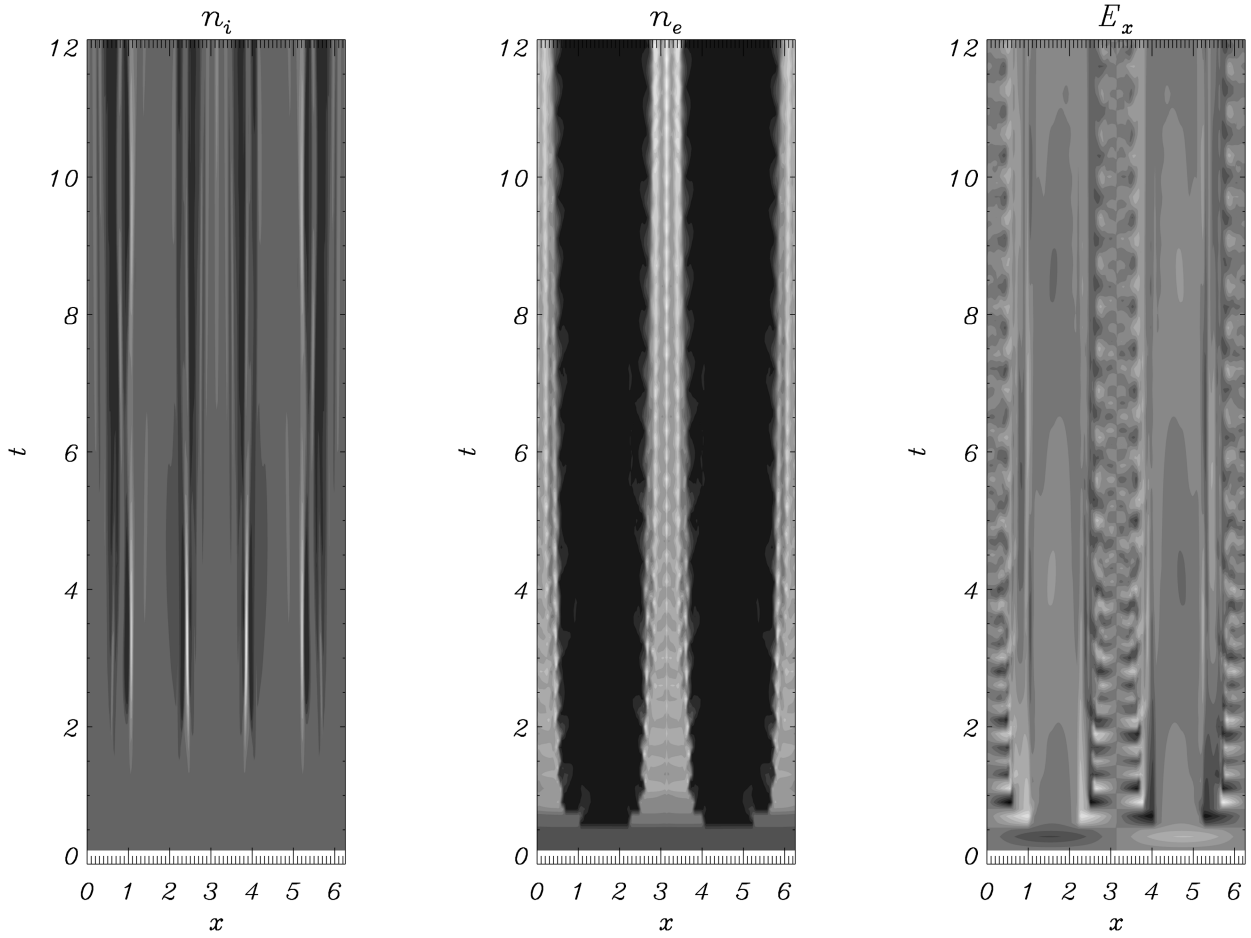

FIG. 8. The shaded contours of the spatial distributions of the ion density, of the electron density, and of the total electric field are shown as functions of x and t, for $\omega_0=10$.

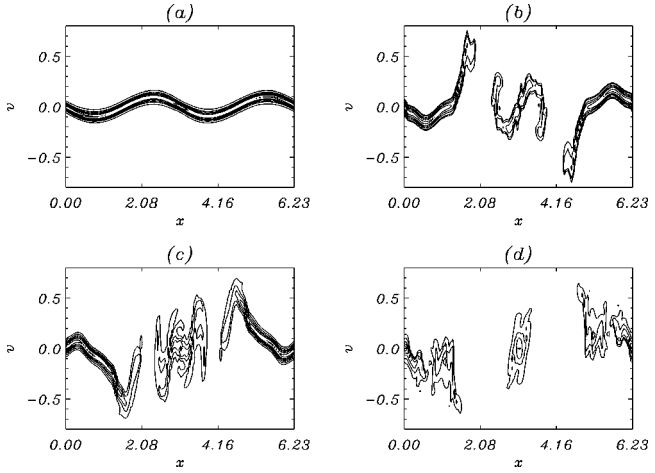

FIG. 9. The isocontours of the electron distribution function $f_e(x,v,t)$ in the phase space (x,v), for $\omega_0=5$. The plots refer to $t=2.7$ (a), 14.5 (b), 15.3 (c), and 30.3 (d).

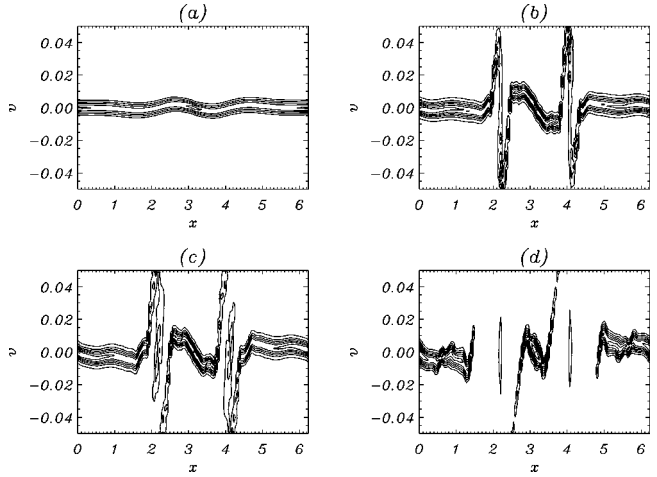

FIG. 10. The isocontours of the ion distribution function $f_p(x,v,t)$ in the phase space (x,v), for $\omega_0=5$. The plots refer to $t=7.5$ (a), 13.4 (b), 16.3 (c), and 30.0 (d).

order of ω_{pi}^{-1}. As a consequence, the ion density can follow the low-frequency oscillation field and the coupling with the electron dynamics is no longer through an average force only. The competition between the ponderomotive force, acting from the high-density side, and the quasistationary one, associated with the slowly varying electric field inside the cavity, determines the motion of the ion fluid. In other words, the common assumption of two well separated time scales, which is often invoked in order to apply the slowly varying envelope approximation to nonlinear problems, breaks down. The ions are piled up ($\delta n_i/n_0<300\%$) exactly at the transition layers between the oscillating and the stationary electric field, because here steep spatial gradients of the electric field are able to maintain ion concentrations which persist stably for tens of the ion plasma times.

For the sake of comparison with the decaying plasma, the electric field k spectrum, $|E_k|^2$, as a function of k and t, is displayed in Fig. 2(b), for $\omega_0=5$. The formation of the externally driven electron cavitation at $t\approx 11$ is accompanied by the sudden appearance of a high-order harmonic content.

Figure 9 displays the electron phase space at $t=2.7$ (a), 14.5 (b), 15.3 (c), and 30.3 (d) for $\omega_0=5$. Here, we have a clearer view of what we have already observed inspecting the phase space of the decaying plasma. A vortex structure typical of the electron trapping inside quasistationary potential wells occurs. It is preceded by the *breaking* of the oscillation which loses its initial regular structure. We also notice that the symmetry which has been introduced in the physical system under consideration by assuming a standing wave, resulting from two counterpropagating ES waves with phase velocities $\pm\omega_0/k$, causes the above discussed electron trapping to be localized around $v=0$. Then, the physical situation can be viewed as if it were produced by two charged particles or particle bunches drifting in opposite directions at velocities $\pm v_0$, much larger than the thermal speed of the background electron population. It would give rise to a sort of one-dimensional electron-electron two-stream instability [19] driven by two charges or localized bunches of charges, instead of two streams. Indeed, the two fast particles would produce two counterpropagating sinusoidal *Cherenkov wakes* of ES oscillations, with wave vectors $\pm k\approx 1/\sqrt{m_e}v_0$. Then the electron trapping shown in Figs. 9(c) and 9(d), corresponding to times of well developed high harmonic content [see Fig. 2(b)], could be interpreted as due to a *nonlinear two-bunch instability* with $v_0\approx 0.3-0.5$. At this point it is worth emphasizing the close similarities between our results and those on the nonlinear evolution of the Buneman instability [20,21]. The concomitant occurrence of the electron trapping, the high harmonic generation, and the spreading of the electron distribution function on one side, and the ion acceleration on the other side, are characteristic of both systems, even if the intensities of the interactions in the two cases are quite different. Another common feature is that the electron drift velocity is much larger than the phase velocity of the electrostatic potential disturbance, the latter being zero in our case.

That the ion dynamics becomes strongly coupled to the electron dynamics in the less dense regions (see Fig. 9) is demonstrated in Fig. 10, where the phase space of the plasma ions is shown at $t=7.5$ (a), 13.4 (b), 16.3 (c), and 30.0 (d) for $\omega_0=5$. We see that the ions undergo *wavebreaking* together

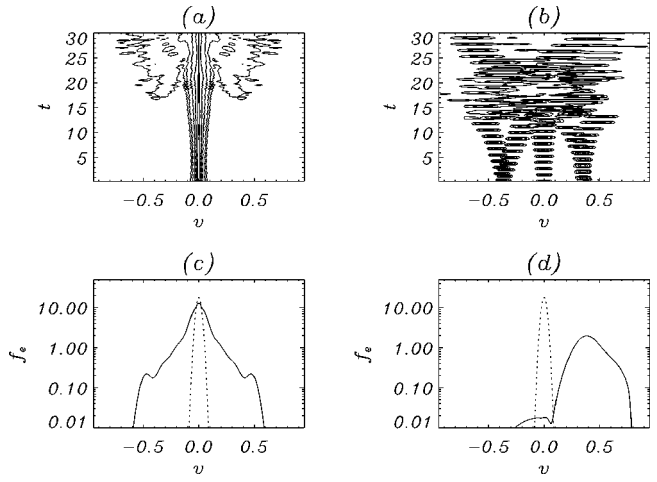

FIG. 11. The electron distribution function $f_e(x,v,t)$ for $\omega_0=5$. The plots are the same as in Fig. 3.

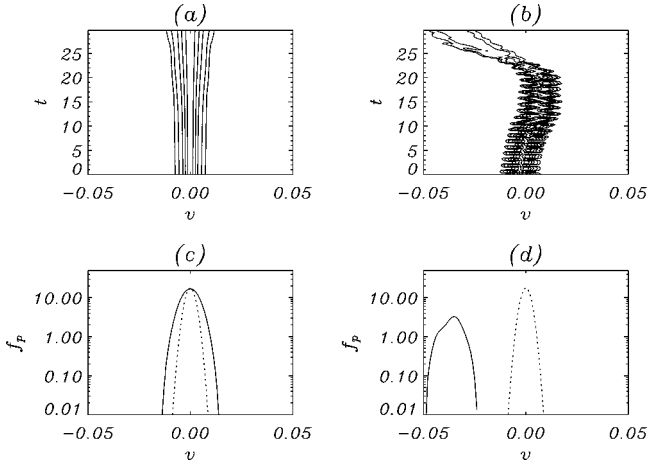

FIG. 12. The ion distribution function $f_i(x,v,t)$ for $\omega_0=5$. The same plots as in Fig. 11 are reported, for $x=0$ [(a) and (c)] and $x=2.6$ [(b) and (d)].

with the electrons right where the plasma density is depressed by the ponderomotive forces. As a consequence, an efficient acceleration of the ions takes place. Various mechanisms of electron and ion acceleration in nonuniform plasmas are described in Ref. [18].

Finally, in Fig. 11, $f_e(x,v,t)$ is shown as in Fig. 3, but for $\omega_0=5$. At $x=0$ [(a) and (c)] the formation of isolated ''beams'' of accelerated electrons is observed, besides the bulk heating as in the case of the decaying plasma. Around $x=\pi/2$ [(b) and (d)] a highly nonequilibrium electron distribution is formed. In order to stress the strong coupling of the electron and ion dynamics in the nonlinear phase of the interaction, we show in Fig. 12 the ion distribution function $f_p(x,v,t)$ for $\omega_0=5$. At $x=0$ [(a) and (c)] the distribution function broadens while maintaining its equilibrium characteristics. On the other side, at $x=2.6$ [(b) and (d)], after an initial phase of forced oscillations at the pump frequency, a low-density ion component starts to be accelerated monotonously acquiring a drift velocity much larger than the ion thermal speed. By inspection of Fig. 5 we can see that this regime occurs in correspondence of the arrival of the ion-density cavity border at the considered coordinate. As discussed above, a quasistationary (negative) electric field is produced locally in these conditions, which turns out to be at the origin of the observed ion acceleration.

V. CONCLUDING REMARKS

This paper contains the results of a detailed (the first, to our knowledge) numerical analysis of the dynamics of a one-dimensional strongly nonlinear electrostatic perturbation in a two-component plasma, paying particular attention to the connections between the phase-space dynamics and the macroscopic evolution of the system. Two cases have been considered: (a) the free decaying of an initial density perturbation and (b) the plasma response to a continuously applied inhomogeneous oscillating electric field, for several values of the pump frequency. Moreover, though remaining in a nonrelativistic regime, we have investigated large amplitude electrostatic perturbations extending to $\tilde{v}^2 \gg v_{Te}^2$, which can characterize low-temperature laboratory or ionospheric plasmas. These regimes, even in the simple one-dimensional case, cannot be treated analytically by any means, but nevertheless they manifest several interesting features and interconnections between the microscopic and the macroscopic behavior of the plasma.

We have demonstrated the quasistationary production of plasma density cavities, the generation of spatial harmonics, and an efficient broadening of the initial electric field spectrum during the interaction. We have observed the transformation of wave energy into electron ''temperature,'' and the production of accelerated particles and the formation of highly nonequilibrium electron distribution functions, depending on the spatial region of observation. Finally, we have shown that the onset of a ponderomotive potential distribution, produced by the rearrangement of the ion density, leads to the process of electron trapping into the potential troughs with the characteristic vortex structure in the phase space.

This analysis, even if limited to a one-dimensional geometry, gives some hints to the experimental investigation both on the strong turbulence and to the wave-particle interaction physics: the electron heating and the frequency downshift of the plasma frequency inside the regions of density depletions, the k-spectral broadening of the initial perturbation, and the fast particle production, on one side, and the electron density accumulation corresponding to the resonant electron trapping inside the wave potential, on the other side, could be subjects of experimental measurements. Notice that, among the several aspects of the interaction mentioned above, the charged particle acceleration experimentally observed during the radiofrequency plasma heating is presently subject to several theoretical interpretations [22].

Moreover, we would like to stress the principal role of the ion dynamics when considering wave-particle interaction in a real plasma. Namely, in a number of papers dealing with the problem of nonlinear Landau damping, as for example Refs. [23,24] among the most recent, the electron dynamics is followed for times of the order of tens or hundreds of times $\sqrt{m_p/m_e}$ of the inverse of electron plasma frequencies, maintaining immobile background ions. In light of our simulations, it appears clear that when an electron-ion plasma is considered, the results drawn in the frame of a fixed-ion model can be changed significantly.

ACKNOWLEDGMENTS

We wish to acknowledge fruitful discussions with and comments by S. V. Bulanov, F. Pegoraro, and V. Petrzilka. Also, we are pleased to acknowledge the Scuola Normale Superiore of Pisa and the supercomputing center of Cineca (Bologna) for the use of their Origin 2000 and Cray T3E computers, respectively. Part of the calculations was performed under an INFM research project at Cineca. One of us (F.C.) is glad to thank I. Lisi (SNS) for numerical suggestions.

[1] V. E. Zakharov, Zh. Eksp. Teor. Fiz. **62**, 1745 (1972) [Sov. Phys. JETP **35**, 908 (1972)].
[2] A. S. Kingsep, L. I. Rudakov, and R. N. Sudan, Phys. Rev. Lett. **31**, 1482 (1973).
[3] K. Nishikawa, Y. C. Lee, and C. S. Liu, Comments Plasma Phys. Control. Fusion **2**, 63 (1975).
[4] O. B. Budneva, V. E. Zakharov, and V. S. Synakh, Fiz. Plazmy **1**, 606 (1975) [Sov. J. Plasma Phys. **1**, 335 (1975)].
[5] V. E. Zakharov, A. F. Mastryukov, and V. S. Synakh, Fiz. Plazmy **1**, 614 (1975) [Sov. J. Plasma Phys. **1**, 339 (1975)].
[6] V. E. Zakharov and L. N. Shur, Zh. Eksp. Teor. Fiz. **81**, 2019 (1981) [Sov. Phys. JETP **54**, 1064 (1981)].
[7] V. V. Krasnosel'skikh and V. I. Sotnikov, Fiz. Plazmy **3**, 872 (1977) [Sov. J. Plasma Phys. **3**, 491 (1977)].
[8] A. S. Lipatov, Pis'ma Zh. Eksp. Teor. Fiz. **26**, 516 (1977) [JETP Lett. **26**, 377 (1977)].
[9] L. M. Degtyarev, R. Z. Sagdeev, G. I. Solov'ev, V. D. Shapiro, and V. I. Shevchenko, Fiz. Plazmy **6**, 485 (1980) [Sov. J. Plasma Phys. **6**, 263 (1980)].
[10] J. G. Wang, G. L. Payne, D. F. DuBois, and H. A. Rose, Phys. Plasmas **1**, 2531 (1994).
[11] J. G. Wang, G. L. Payne, D. F. DuBois, and H. A. Rose, Phys. Plasmas **2**, 1129 (1995).
[12] F. Califano and M. Lontano, Phys. Scr. **T75**, 208 (1998).
[13] R. Cesario, R. Bartiromo, A. Cardinali, F. Paoletti, V. Pericoli-Ridolfini, and R. Schubert, Nucl. Fusion **32**, 2127 (1992).
[14] H. L. Pecseli, K. Iranpour, O. Holter, B. Lybekk, J. Holtet, J. Trulsen, A. Eriksson, and B. Holback, J. Geophys. Res. **101**, 5299 (1996).
[15] C. Castaldo, E. Lazzaro, M. Lontano, and A. M. Sergeev, Phys. Lett. A **230**, 336 (1997).
[16] A. Mangeney, F. Califano, E. Fijalkow, L. Nocera, and G. Einaudi (unpublished).
[17] F. Califano, F. Pegoraro, S. V. Bulanov, and A. Mangeney, Phys. Rev. E **57**, 7048 (1998).
[18] S. V. Bulanov, L. M. Kovrizhnykh, and A. S. Sakharov, Comments Plasma Phys. Control. Fusion **11**, 183 (1988); also Phys. Rep. **186**, 1 (1990).
[19] C. K. Birdsall and A. B. Langdon, *Plasma Physics Via Computer Simulation* (McGraw-Hill, New York, 1985), Sec. 5.9.
[20] O. Ishihara, A. Hirose, and A. B. Langdon, Phys. Rev. Lett. **44**, 1404 (1980).
[21] O. Ishihara, A. Hirose, and A. B. Langdon, Phys. Fluids **24**, 452 (1981).
[22] V. Petrzilka, V. Fuchs, L. Krlin, J. A. Tataronis, M. Lontano, P. Pavlo, and F. X. Soeldner, in *Proceedings of the Second Europhysics Topical Conference on Radio Frequency Heating and Current Drive of Fusion Devices*, edited by J. Jacquinot, G. Van Oost, and R. R. Weynants, Europhysics Conf. Abs. Vol. 22A (European Physical Society, Brussels, 1998), p. 149.
[23] M. B. Isichenko, Phys. Rev. Lett. **78**, 2369 (1997).
[24] G. Manfredi, Phys. Rev. Lett. **79**, 2815 (1997).